Int. J. Dev. Biol. 46: 755-763 (2002)

Original Article

Developmental patterning of the circumvallate papilla

SUWANNA JITPUKDEEBODINTRA, YANG CHAI and MALCOLM L. SNEAD*

Center for Craniofacial Molecular Biology, School of Dentistry, University of Southern California, Los Angeles, USA

ABSTRACT Organogenesis is regulated by the sequential and reciprocal interactions between epithelial and mesenchymal tissues. Many molecules, including growth factors, transcription factors, extracellular matrices, cell surface receptors, and matrix degrading enzymes, have been found to be involved in this process. To investigate the molecular mechanism responsible for morphogenesis of the circumvallate papilla/von Ebners' gland complex, we examined the expression patterns of selected cell adhesion molecules, extracellular matrix molecules, innervation and cell division in the circumvallate papilla of mouse embryos from embryonic day 11.5 (E11.5) to E14. At E11.5-E13.5, the lingual epithelium, the site where the circumvallate papilla will develop, is negative for BrdU labeling. At E14-E15, we detected cell division in the papillary area, especially in the epithelial invagination where von Ebners' minor salivary gland will form. The basement membrane component, laminin, is expressed as a continuous thin line separating the epithelia from the underlying mesenchyme, but it is broadly and strongly expressed in the area where the nerve fibers penetrate into the circumvallate papilla. At the E12-E12.5 stage of development, the epithelial thickening shows intense E-cadherin staining in the superficial and basal layers, but weak E-cadherin staining in the suprabasal layer. E-cadherin is strongly expressed, but appears dispersed among the basal layer of lingual epithelium, the site where nerve fibers will innervate. At E13, nerve fibers reach the circumvallate papilla. These nerve fibers penetrate into and split the epithelial cell mass into two stalks which will later differentiate to form the von Ebners' gland. These results suggest that 1) the formation of the circumvallate papilla does not initially depend on cell division, 2) cell migration likely plays a major role during circumvallate placode formation, 3) E-cadherin and laminin may play a role in nerve guidance and 4) innervation impacts the final morphogenesis of the circumvallate papilla.

KEY WORDS: *circumvallate papilla, E-cadherin, laminin, PGP 9.5, morphogenesis*

Introduction

Morphogenesis and cytodifferentiation in developing vertebrate organs is controlled by the sequential and reciprocal interactions between epithelial and mesenchymal tissues. During the early stage of morphogenesis, many organs share common morphological features that begin with the thickening of an epithelial sheet, followed by invagination of the epithelia into the underlying mesenchyme. With advancing morphogenesis and cytodifferentiation, such as folding and/or branching of epithelia or secretion of cell specific products, epithelial and mesenchymal interaction is critical for mediating the signal(s) exchanged during each developmental process. Ultimately, these interaction(s) will give rise to different types of organs, such as hair/feather, scale, tooth, limb, kidney, and glands (Chuong, 1993; Jernvall and Thesleff, 2000; Warburton *et al.*, 2000).

The tongue is an organ that is subject to pattern formation with unique rostral-caudal and dorsal-ventral characteristics, as well as striking morphogenetic identity (Jung *et al.*, 1999). Gustatory papillae are one of the specialized and complex structures found on the dorsal surface of the tongue. Due to the presence of taste buds, the epithelia of the gustatory papillae are distinguished from adjacent tongue epithelia. Taste buds contain sensory cells for the chemical sense of taste and require innervation to convey sensory information to the central nervous system. There are three types of gustatory papillae in mammals distributed in a rostral-caudal axis. The fungiform papillae are distributed on the anterior two-thirds of the tongue, the foliate papillae are found at the junction of the anterior two-thirds and the posterior one-third of the tongue, and the circumvallate papilla are found in the posterior one-third of the tongue. The molecular mechanism that directs the rostral-caudal axis and hence directs papilla formation, growth, and maintenance is not well understood (Jung *et al.*, 1999).

Abbreviations used in this paper: BrdU, bromodeoxyuridine; CVP, circumvallate papilla; E, embryonic; ECM, extracellular matrix; VEG, von Ebners' gland.

***Address correspondence to:** Dr. Malcolm L. Snead. Center for Craniofacial Molecular Biology, School of Dentistry, University of Southern California, 2250 Alcazar Street, CSA 103, Los Angeles, CA 90033, USA. Fax. +1-323-442-2981. e-mail: mlsnead@usc.edu

0214-6282/2002/$25.00

Printed in Spain
www.ijdb.ehu.es

The circumvallate papillae (CVP) differ from other gustatory papilla. They contain progenitor cells that may differentiate into taste buds, and into serous cells in a tubulo-acinar salivary gland, von Ebners' gland (VEG). Because of this unique developmental pathway, the organ provides an insightful model for the study of patterning and cell-differentiation during organogenesis. CVP number varies across species; 9-13 in human, 1 in mouse and rat, and 2-3 in rabbit, pig and horse (Spielman and Brand, 1995). Mouse CVP forms initially from the thickening of dorsal epithelia in the middle of the posterior one-third of the tongue between embryonic day-11 and -12 (E11 and E12). This placode will later be innervated bilaterally by the nerve fibers from the glossopharyngeal nerve and acquire a mesenchymal core forming a "dome-shaped" structure with two adjacent epithelial stalks. These two stalks invaginate into the underlying mesenchyme, and give rise to the von Ebners' minor salivary gland. The sequence of developmental events from the earliest placode formation, through cytodifferentiation, to finally forming the adult structure, is similar to other placode-derived structures such as hair, teeth and whiskers (Iseki *et al.*, 1996; Thesleff *et al.*, 1996). However, to undergo terminal cytodifferentiation to form taste cells responsive to chemical stimuli, the gustatory papillae requires innervation that other placode-dependent organs do not (Thesleff *et al.*, 1990; Farbman and Mbiene, 1991; Oakley, 1993; Oakley *et al.*, 1993; Mbiene *et al.*, 1997; Morris-Wiman *et al.*, 1999).

In this study we correlate the expression pattern of cell adhesion molecule and extracellular matrix molecule with the changes in CVP morphology and innervation during CVP initiation and morphogenesis. These investigations are an initial step towards the understanding of regulatory roles of cell-cell and cell-matrix interactions during CVP development.

Results

Morphogenesis of Circumvallate Papilla (CVP) in the Mouse

At embryonic day 11.5 (E11.5), the two lateral lingual swellings of the anterior portion of the tongue are separated from the posterior portion of the tongue by a deep sulcus. The dorsal lingual epithelial surface bears no morphological evidence of CVP formation. However at the microscopic level, a broad thickening of the dorsal tongue epithelia can be seen in the middle posterior one-third of the tongue where the CVP will form (Fig. 1A). At E12 and E12.5, the tongue is now recognizable. The broad epithelial thickening becomes more localized at the midline and is distinguished as a 10-20 cells thick placode (Fig. 1B). From E13 to E14, the CVP placode expands into the underlying mesenchyme. Starting from E13 to E14, CVP morphology is dramatically changed from a placode-like structure into a "dome-shaped" structure. At E13, three different morphologies are observed. In the posterior aspect (see line C, Scheme 1) of E13-E14, the CVP placode evaginates to form a "ball" of tissue, (Fig. 1C) while in the middle aspect (see line B, Scheme 1), CVP forms a "ring-like" structure (see Fig. 4 C,D) and/or a "dome-shaped" structure with a loose-tissue core (Fig. 1D). However, at the anterior aspect (see line A, Scheme 1), the CVP remains as a placode-like structure (Fig. 1E). From E15-E16, a "ball" of cells at the posterior portion and the "ring-shaped" structure at the middle portion of the CVP disappear, leaving only the "dome-shaped" structure with its mesenchymal core (Fig. 1F). The epithelium overlying the "dome" of the CVP becomes thinner, about 3-5 cells

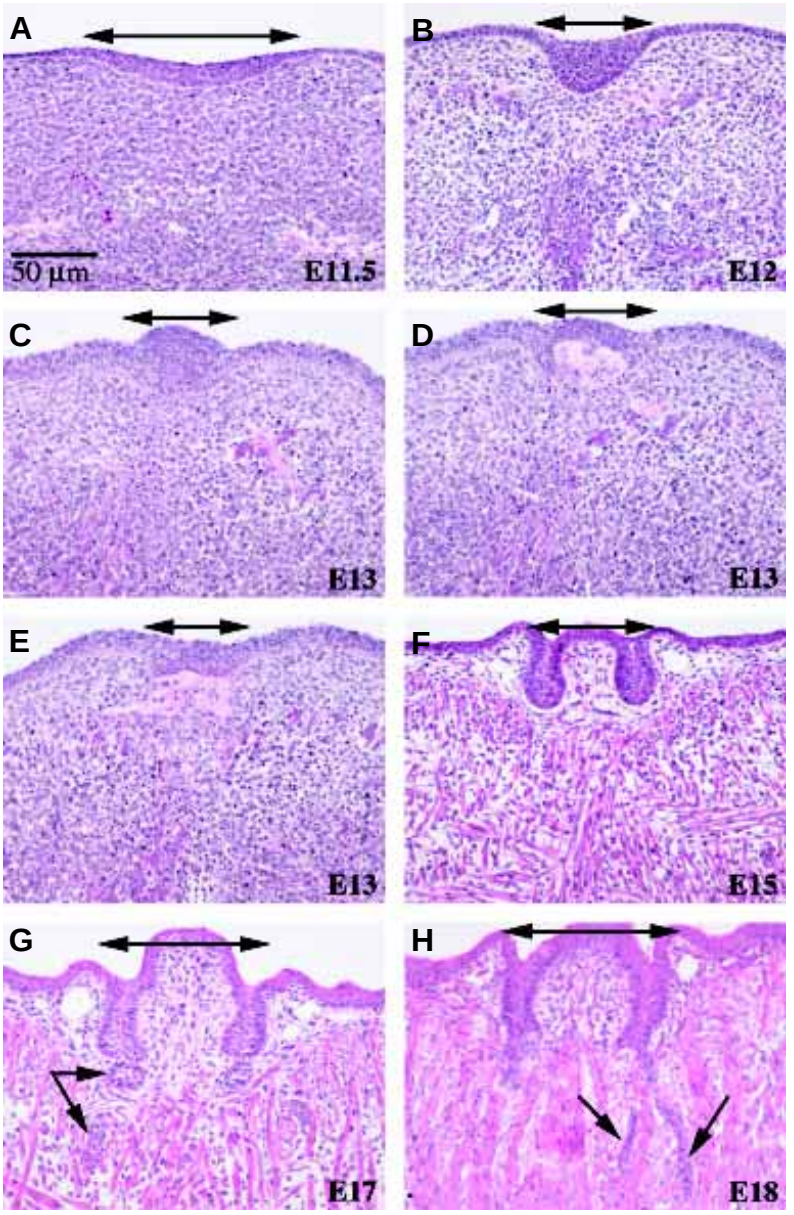

Fig. 1. H&E staining of mouse embryonic CVP from E11.5-E18. *The double arrow defines the CVP at each developmental stage.* **(A)** *At E11.5, the CVP is first detectable as a broad epithelial thickening.* **(B)** *At E12, epithelial thickening condensed in the midline. (C-E) From E13 to E14, the CVP forms a "ball-like" structure at the posterior end* **(C)**, *a "dome-like" structure in the middle portion* **(D)** *and a "placode-like" structure at the anterior portion* **(E)**. **(F)** *From E15-E16, a "dome-like" structure with two epithelial stalks remains.* **(G)** *At E17, the two epithelial stalks invaginate deeply into the underlying mesenchyme (arrows).* **(H)** *At E18, branching morphogenesis of von Ebners' gland starts (arrows). Bar, 50 µm for all images.*

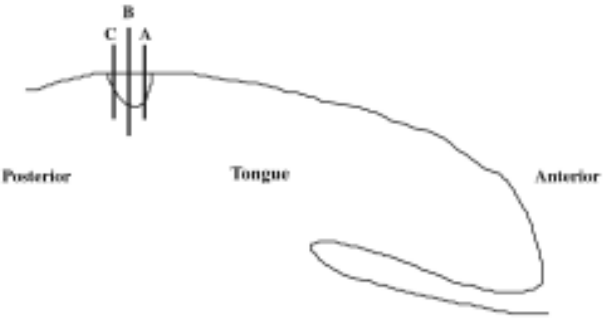

Scheme 1. Plane of sections used in this study. *The anterior (A), middle (B) and posterior (C) portions of the CVP.*

thick, and at the base of the "dome" two stalks are formed. At E17, these two stalks invaginate deeply into the tongue mesenchyme (Fig. 1G). These two invaginations will later contribute to the von Ebners' minor salivary gland (VEG). By E18 of development, branching morphogenesis of VEG is observed (Fig. 1H).

Cell Proliferation Activity during CVP Development

BrdU incorporation was used to detect cell proliferation within the CVP placode from developmental stages E11.5 to E15. From E11.5-E12.5, BrdU-labeled cells are distributed generally in both the tongue mesenchyme and the epithelium. However the epithelial placode of the CVP is spared from labeling (Fig. 2 A-C). At E13, a few BrdU-positive cells are observed within CVP core (arrowhead in Fig. 2D). At E13.5, a few cells of the epithelial "dome" (arrows in Fig. 2E) and the cells inside the mesenchymal core (arrowhead in Fig. 2E) are BrdU-labeled. At E14 and E15, BrdU-labeling remains largely negative in the epithelia on the roof of the "dome", but there are BrdU-positive cells found at the invaginating stalks at the base of the "dome" (arrows in Fig. 2 F,G). These two stalks will later invaginate and undergo development to form the paired von Ebners' minor salivary gland (see Fig. 1 G,H).

Localization of Laminin

In this study we examined the changing distribution of laminin during CVP morphogenesis and innervation. At E11.5 laminin is present as a continuous thin line separating the tongue epithelium from the underlying mesenchyme (data not shown). Laminin immunoreactivity is also found in the basement membrane of the nerves and blood vessels in the tongue at all stages examined in this study (see asterisks in Fig. 3 A-C).

The localization of laminin at E12.5 CVP placode is similar to the laminin distribution observed at E12. At the posterior portion (see line C, Scheme 1) and also in the area anterior to E12 and E12.5 CVP placode (anterior to line A, Scheme 1), laminin is distributed in the basement membrane as a continuous thin line separating the tongue epithelia from the underlying mesenchyme (data not shown). In the area closest to the anterior portion (see line A, Scheme 1) of E12 and E12.5 CVP placode, the localization of laminin is broad and extends from the cells along the basement membrane into the cells positioned well above the basement membrane (arrows in Fig. 3A). In the middle portion of E12.5 CVP placode, laminin immunodetection is weaker, but remains traceable, in the area where nerves almost reach the basement membrane (arrows in Fig. 3B).

At the posterior portion (see line C, Scheme 1) of E13 and E13.5 CVP, laminin is distributed as a continuous line clearly separating epithelia from underlying mesenchyme (data not shown). In the area where the "ring-shaped" structure forms, a broadening of laminin immunostaining in the epithelial cells in the middle of the "ring" and in some cells on the top of the "ring" surface are observed (arrows in Fig. 3C). At the area closest to the "dome-shaped" structure, we observed three different laminin immunostaining patterns. First, laminin is surrounded the central core of the "ring" and is broadly distributed at the opening site where the epithelial cell mass will separate to form the "dome-shaped" structure (arrow in Fig. 3D). Second, laminin immunostaining is found surrounded the central core and there are two broad area of laminin immunoreactivity extending from middle of the "ring" to the basement membrane of CVP at both sides of the opening area of the "ring" (arrows in Fig. 3E). Lastly, laminin is observed as two broadly defined areas at the right and left sides of the CVP placode (arrows in Fig. 3F). At the "dome-

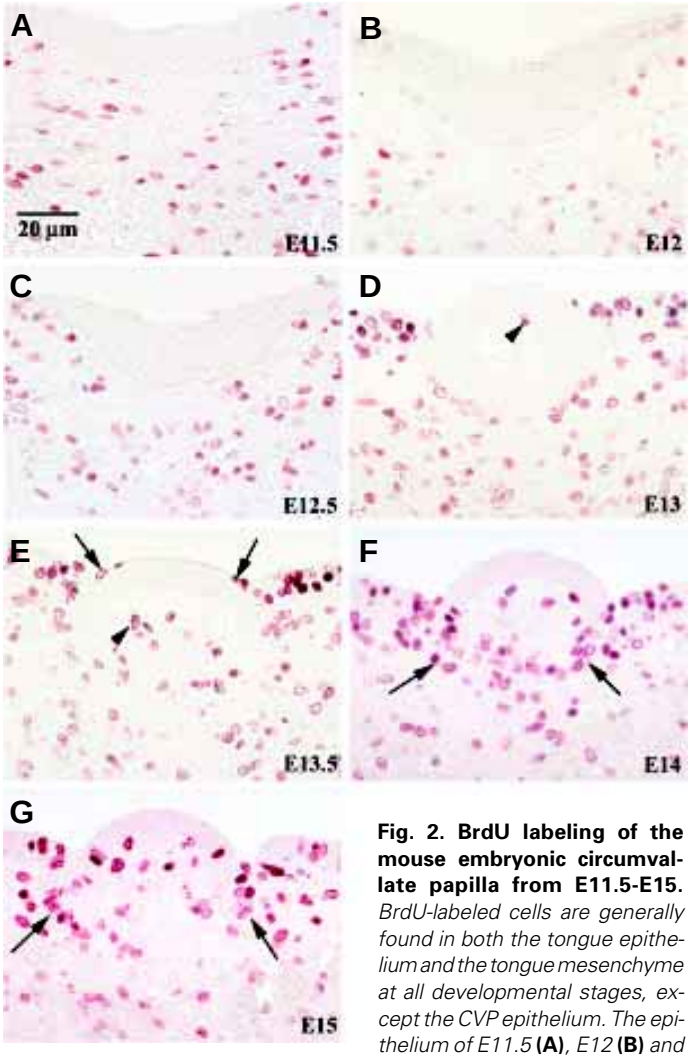

Fig. 2. BrdU labeling of the mouse embryonic circumvallate papilla from E11.5-E15. *BrdU-labeled cells are generally found in both the tongue epithelium and the tongue mesenchyme at all developmental stages, except the CVP epithelium. The epithelium of E11.5* **(A)**, *E12* **(B)** *and E12.5* **(C)** *of the CVP epithelial placode are spared from labeling.* **(D)** *At E13, the entire CVP epithelium remains negative for BrdU-labeling, but a few BrdU-positive cells are observed in the mesenchymal core (arrowhead).* **(E)** *At E13.5, a few cells of the CVP epithelial "dome" (arrows) and the cells in the mesenchymal core (arrowhead) are BrdU-labeled. At E14* **(F)** *and E15* **(G)**, *BrdU-labeling remains negative in the epithelia on the top of the "dome", but BrdU-labeled cells are found in the invaginating stalks (arrows). Bar, 20 μm for all images.*

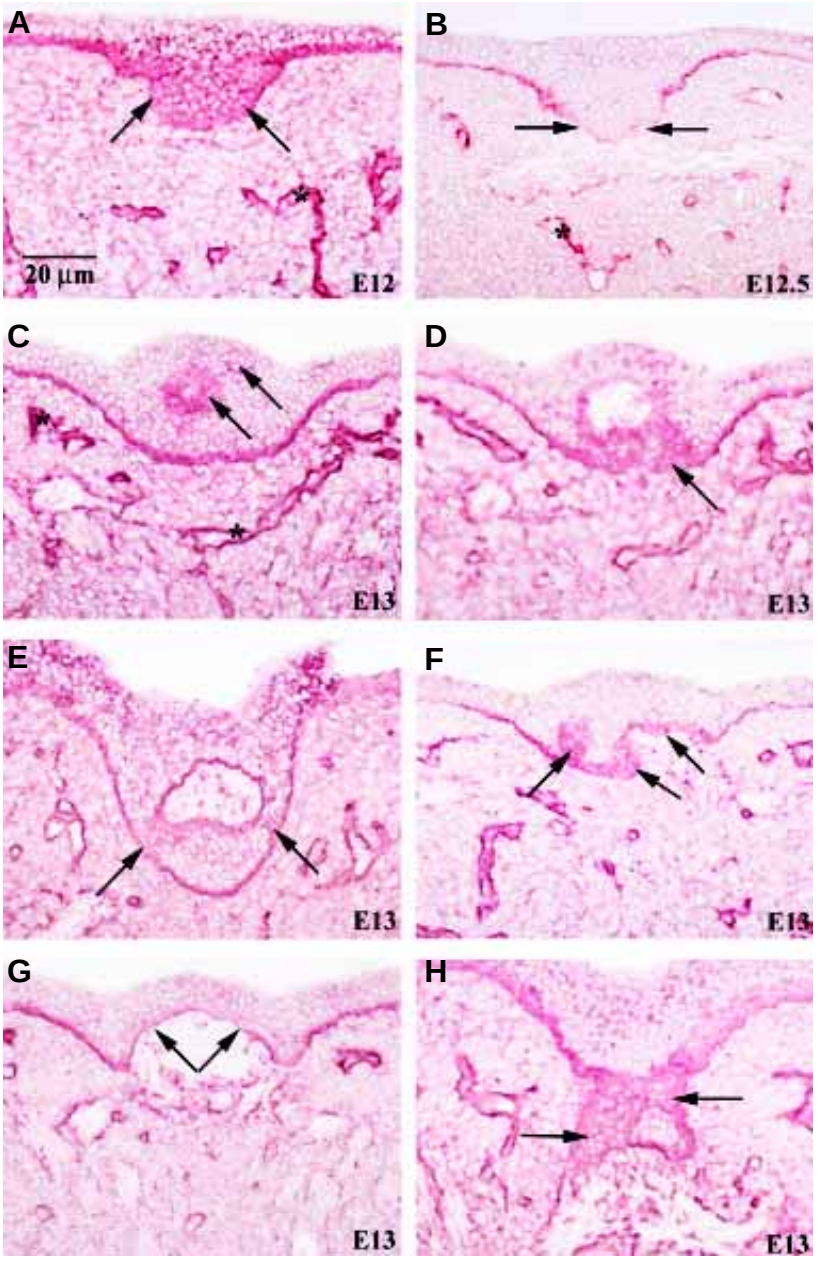

Fig. 3. Immunohistochemical detection of laminin from E12-E13 of the developing CVP. *Laminin immunoreactivity is intensely distributed as a continuous thin line along the basement membrane at the posterior end of the E12 and E12.5 CVP placode (data not shown) and also along the basement membrane of blood vessels (asterisks).* **(A)** *In the area closest to the anterior end of the E12 CVP placode, laminin is expressed irregularly and broadly extending from the cells along the basement membrane to the cells positioned well above the basement membrane (arrows).* **(B)** *In the middle portion of the E12.5 CVP placode, at the site where nerves approach the basement membrane, laminin immunoreactivity is very weak, but remains traceable (arrows).* **(C)** *At the "ring" area of the E13 CVP, laminin is broadly distributed among the epithelial cells at the middle of the "ring" and in some epithelial cells on the top of the "ring" surface (arrows).* **(D-F)** *In the middle portion of the E13 CVP, laminin is broadly distributed in the area where the epithelia separated to form a "dome" structure (arrow in D), or laminin immunostaining is extended from the middle of the "ring" to the basement membrane at both sides of the opening area (arrows in E) or laminin is broadly distributed at the left and the right sides of the CVP placode (arrows in F).* **(G)** *In the "dome" shaped area of the E13 CVP, laminin is distributed as a continuous thin line along the basement membrane (arrows).* **(H)** *At the area closest to the anterior end of the E13 CVP, laminin is broadly distributed and extends from the basement membrane toward the cells positioned well above the basement membrane (arrows). Bar, 20 μm for all images.*

shaped" area, laminin is distributed as a continuous line along the basement membrane (arrows in Fig. 4G). At the area closest to the anterior end (see line A, Scheme 1) of the CVP placode, laminin is broadly distributed and extends from the cells along the basement membrane to among the cells positioned well above the basement membrane of the placode (arrows in Fig. 4H). In the area anterior to the E13 CVP placode, laminin is distributed as a continuous line along the basement membrane (data not shown).

Localization of E Cadherin

To determine the expression profiles of E-cadherin during CVP morphogenesis and innervation, we performed immunohistochemistry on mouse CVP at developmental stages E12-E13.5. The localization of E-cadherin at E12.5 CVP placode is similar to the distribution observed at E12. At the posterior end (see line C, Scheme 1) of the E12-E12.5 CVP placode, E-cadherin is intense in the epithelial cells from the basement membrane toward the epithelial cells in the superficial layer (data not shown). At the anterior end (see line A, Scheme 1) of the CVP placode, E-cadherin is intense in all cell layers (Fig. 4A). However, the staining in the epithelial cells at the tip of placode along the basement membrane is diffuse and the demarcation between the epithelia and the mesenchyme is poorly defined (arrows in Fig. 4A). In the middle portion (see line B, Scheme 1) of the E12 (data not shown) and E12.5 CVP placode, E-cadherin is most intense in the superficial epithelial cell layer and in the epithelial cells along the basement membrane (arrows in Fig. 4B). However, the E-cadherin immunostaining is decreased in the epithelial cells located in the middle layer of the placode (arrowhead in Fig. 4B).

Expression patterns of E-cadherin at E13 and E13.5 are similar. At the posterior end (see line C, Scheme 1) of E13 and E13.5 CVP, E-cadherin immunoreactivity is decreased gradually from the superficial cell layer to the basal cell layer: being most intense in the epithelial cells along the superficial layer and less intense in the epithelial cells along the basement membrane (data not shown). At the "ring" area, E-cadherin immunostaining is intense in the cells that define the middle of the "ring" and the superficial layer (arrows in Fig. 4C), but the staining is weaker among the epithelial cells positioned between these two layers as well as the cells near the basement membrane (arrowheads in Fig. 4C). Staining of E-cadherin in the "ring" area where the nerve will penetrate into the CVP is intense and of approximately equal intensity among all cell layers from the middle cell layer of the "ring" toward the basement membrane (arrow in Fig. 4D). At the "dome" area, E-cadherin staining is very intense in the

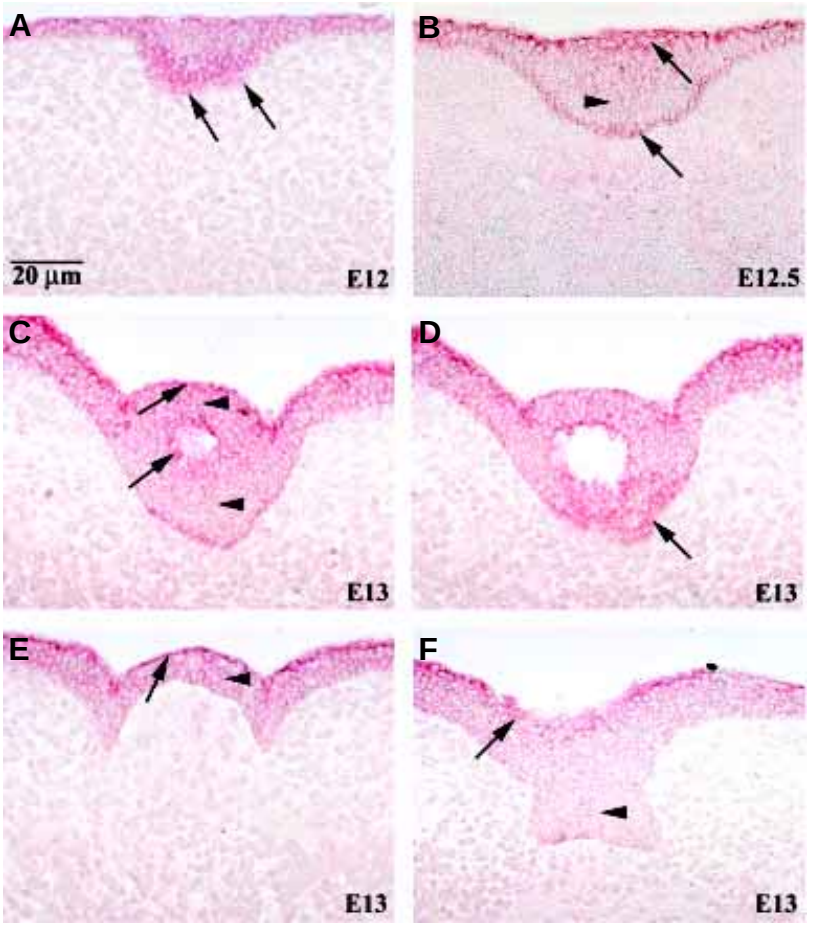

Fig. 4. Immunohistochemical detection of E-cadherin from E12-E13 of the developing CVP. (A) *At the anterior end of the E12 CVP placode, E-cadherin staining is intense but appears diffuse in the epithelial cells at the tip of the placode (arrows).* **(B)** *At the middle portion of the E12.5 CVP placode, E-cadherin is most intense in the epithelial cells in the superficial and the basal cell layers (arrows), but very weak in the epithelial cells in the middle layer of the placode (arrowhead).* **(C)** *In the "ring" structure of the E13 CVP, E-cadherin staining is intense in the superficial epithelial cell layer and in the epithelial cells at the middle of the "ring" (arrows). However, the staining is very weak in the epithelial cells positioned between these two layers as well as among the epithelial cells near the basement membrane (arrowheads).* **(D)** *E-cadherin staining is also intense in the epithelial cells of the "ring" area at the site where the nerve will penetrate into the E13 CVP (arrow).* **(E)** *In the "dome" area, E-cadherin staining is intense in the superficial epithelial cell layer (arrow) but is weaker in the epithelial cells near the basement membrane (arrowhead).* **(F)** *At the anterior end, E-cadherin staining is most intense in the superficial epithelial cell layer (arrow) but is absent in the epithelial cell mass closest to the basement membrane (arrowhead). Bar, 20 µm for all images.*

superficial cell layer (arrow in Fig. 4E) although the staining is weaker in the cells along the basement membrane (arrowhead in Fig. 4E). At the anterior portion (see line A, Scheme 1) of E13 CVP, the staining is most intense in the superficial layer (arrow in Fig. 4F) but is absent in the cell mass closed to the basement membrane (arrowhead in Fig. 4F). Anterior to the CVP placode, E-cadherin staining is intense in all cell layers (data not shown).

Innervation of Developing Circumvallate Papilla

The innervation of developing circumvallate papilla was examined using the pan-neuronal antibody directed against ubiquitin carboxyl terminal hydrolase (protein gene product 9.5; PGP 9.5) (Thompson *et al.*, 1983). We observed nerve fibers in the mandibular process starting from E11.5, but the nerve fibers remain distant from the tongue epithelium (data not shown). At E12 and E12.5 nerve fibers penetrate closer to the tongue epithelium but have not yet reached the tongue epithelium (arrows in Fig. 5 A,B). At E13, the neuronal markers were detected in the middle of the "ball-like" cell mass (arrow in Fig. 5C), in the middle of the "ring-shaped" structure (arrow in Fig. 5D), in the central core of the "dome" (arrow in Fig. 5E), as well as the mesenchymal cells beneath the anterior end of CVP placode (arrow in Fig. 5F). We did not detect this neuronal marker in nerve fibers in the CVP epithelium until E14 (arrows in Fig. 5G). At E 15, the central core of the CVP is filled densely with nerves and additional nerves in the CVP epithelium are detected (arrow in Fig. 5H).

Contribution of Cranial Neural Crest Cells during CVP Development

To clarify whether the neural crest-derived cells contribute to the CVP placode formation, the *Wnt 1-Cre*/R26R reporter mice are used to monitor neural crest-derived cell lineages during CVP development. All of the blue-stained cells showed in Fig. 6 are neural crest-derived cells, whereas the cells lacking X-gal staining are non-neural crest-derived. We found that the mesenchymal cells underlying the CVP, within the core of the CVP and also the nerve supply to the CVP is neural crest-derived (Fig. 6 A-F).

Discussion

The development of the circumvallate papilla resembles other systems of organogenesis, such as feather, hair, lung, mammary gland and tooth (Chuong, 1993; Jernvall and Thesleff, 2000; Warburton *et al.*, 2000). These regulated developmental processes involve complex sequential and reciprocal interactions between epithelia and mesenchymal tissues. However, the developmental program for each distinct organ requires tissue-specific regulatory factors and signaling pathways. So far, little is known about the molecular regulatory mechanism during pattern formation of the tongue or circumvallate papilla (Hall *et al.*, 1999; Jung *et al.*, 1999). In order to better understand the development of the CVP, we examined markers of cell division, cell adhesion, a basement membrane component, neural tissue, and neural crest cell-derivatives.

The embryonic stage demarcating the first morphological sign of CVP formation in our study differs from that stage previously reported by Paulson *et al.* (1985) and AhPin *et al.* (1989). Paulson *et al.* (1985) observed the first histological indicator for CVP formation in CD-1 mouse fetuses at E14. However, AhPin *et al.* (1989) first observed CVP formation in Balb/c mouse fetuses at E13. In our study, we used Swiss Webster (SW) mouse, an outbreed strain, as an animal model. The first histological indicator of CVP formation in SW mice was seen as early as E11.5, starting

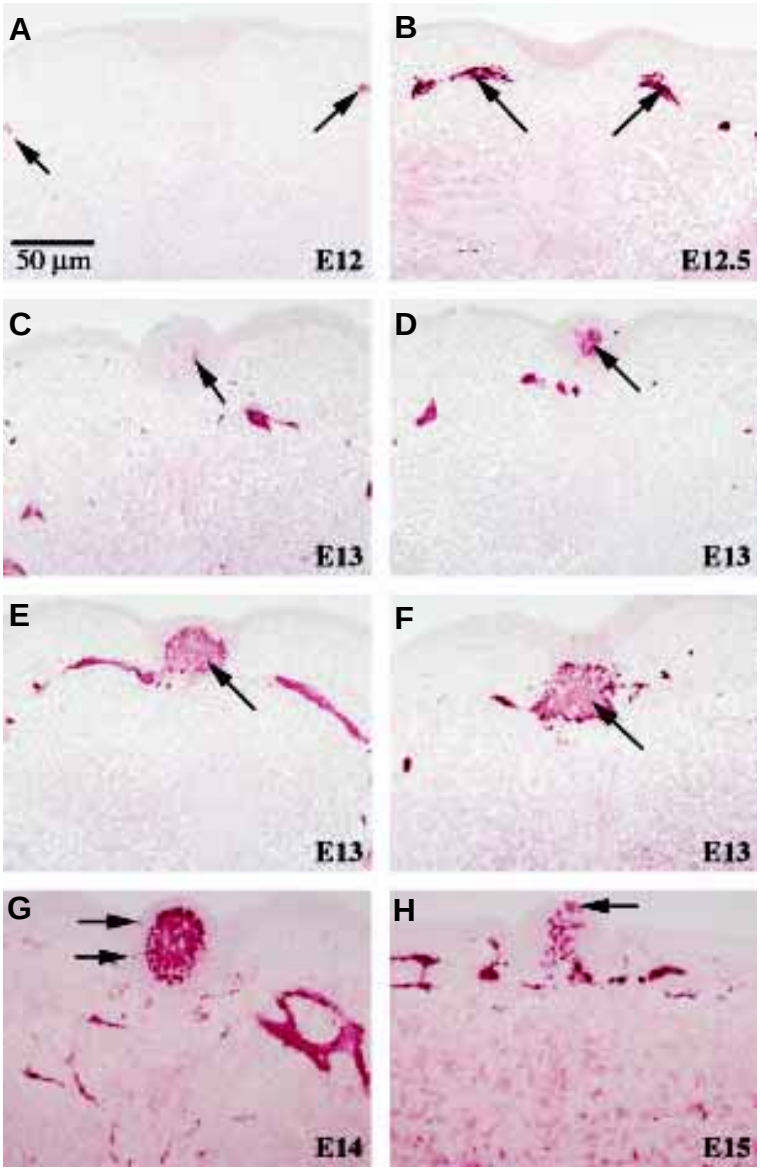

Fig. 5. Immunohistochemical detection of the nerve tissue marker PGP 9.5, in the developing CVP from E12 to E15. (A) *At E12, nerve fibers are found in the tongue but remain distant from the tongue epithelium (arrows).* **(B)** *At E12.5, nerve fibers approach the CVP epithelial placode (arrows).* **(C)** *At the posterior end of the CVP at E13, the marker for the neuronal tissue is detected in the middle of the "ball-like" cell mass (arrow).* **(D)** *At E13, in the area where the "ring" structure forms, the marker for the neuronal tissue fills in the middle of the "ring" (arrow).* **(E)** *At E13, in the area where the "dome-like" structure forms, the marker for the neuronal tissue fills in the central core of the dome (arrow).* **(F)** *At the anterior end of E13 CVP, the marker for the neuronal tissue is found beneath the cell mass of the CVP placode (arrow).* **(G)** *At E14, the neuronal marker is detected in the central core of the CVP "dome" and also within the CVP epithelium (arrows).* **(H)** *At E15, the neuronal marker within the CVP epithelium is detected (arrow). Bar, 50 μm for all images.*

as a broad thickening of dorsal epithelia of the tongue, a developmental stage slightly earlier than that previously reported (Paulson *et al.*, 1985; Ahpin *et al.*, 1989). At E12, a developmental stage equivalent to E13 of those observed by AhPin *et al.* (1989), the broad thickening epithelia became more restricted and condensed in the middle of the posterior one-third of the tongue. These discrepancies in temporal events are likely due largely to differences in murine strains.

The earliest stage of CVP formation starts as a broad thickening of epithelial cells and at latter developmental stages, these cells accumulate and condense in the middle of the tongue as a distinct placode. At E13, innervation and CVP morphogenesis begins. There are three possibilities to explain how epithelial thickening forms a placode; 1) cell division, 2) cell migration, or 3) mesenchymal-epithelial transformation (de Iongh, *et al.*, 2001). In our study, we used BrdU as a marker to label dividing cells during early CVP placode formation. However, we did not detect BrdU-labeled cells in the epithelial placode from E11.5 to E13. At E13.5 to E14, BrdU incorporation remained negative on the top of the CVP "dome". However, we detected a few BrdU-positive cells in the epithelial invagination area that will later form von Ebners' gland as well as BrdU incorporation into cells within the mesenchymal core of the CVP (see Fig. 2). We interpret the negative BrdU-labeling cells in the CVP placode as an indication that cell division does not directly participate in epithelial thickening during the earliest stage of CVP placode formation.

The other possibility underlying epithelial thickening is that the cells in the placode might derive from mesenchymal-epithelial transformation. A mesenchymal to epithelial transformation occurs normally during development such as during somite formation, vasculogenesis or nephrogenesis (Ekblom, 1989; Barasch, 2001). We used a *Wnt1-cre*/R26R reporter mouse model to identify and thereby to follow the lineages of neural crest cell population within the CVP. The proto-oncogene *Wnt1* is expressed in the developing central nervous system and also in the neural crest cell population emigrating from the neural tube (Wilkinson *et al.*, 1987; Echelard *et al.*, 1994). The R26R reporter mouse exhibits constitutive β-gal expression in all cells during embryonic development when crossed with ubiquitously expressed *cre* (Friedrich and Soriano, 1991; Zambrowicz *et al.*, 1997). Cross mating between the *Wnt1-cre* transgenic mouse with the R26R reporter mouse created double transgenic line in which lac Z expression is restricted to progenitors of the neural crest cells. In our study, we found no lac Z positive cell in the epithelial placode area. We interpret the absence of a neural crest-derived contribution to the placode as an evidence that mesenchymal-epithelial transformation does not play a significant role in the formation of the CVP placode.

The remaining possibility is that placode thickening occurs as a result of cell migration. To test this hypothesis, we examined one of the cell adhesion molecules to see if it was altered during placode thickening. In this study we demonstrated the heterogeneous distribution of E-cadherin during CVP morphogenesis. E-cadherin was intensely expressed in the superficial and basal epithelial cell layers during CVP placode formation. However E-cadherin expression decreased in the epithelial cells within the middle cell layer of the placode (as shown in Fig. 3B). At E13 when CVP morphogenesis and innervation occur, E-cadherin was strongly expressed in the superficial cell layer, in the middle of the CVP "ring" and at the site where nerve processes penetrated into the CVP placode. However, E-cadherin decreased in the cells closest to the basement membrane (as shown in Fig. 3 C-F).

E-cadherin is a member of the cadherin family of transmembrane Ca^{2+}-dependent, homotypic cell adhesion molecules, which mediates cell adhesion, as well as being regulated during cell movement. In adult tissues, E-cadherin remains expressed at high levels and participates in maintaining tissue architecture (Gumbiner, 1996). The loss of E-cadherin expression can lead to increased cell motility, such as during invasive or metastasis of epithelial tumors (Frixen *et al.*, 1991), cell migration/rearrangement and during epithelial-mesenchymal transformation during normal developmental processes (Shuler *et al.*, 1992; Sjodin *et al.*, 1995). In this study, the observed decrease in E-cadherin expression in a particular subset of epithelial cells in the CVP placode and in the cells closest to the basement membrane when innervation initiates, is consistent with epithelial cells undergoing migration and rearrangement (Gumbiner, 1996). The strong expression of E-cadherin in the superficial cell layer, the cells surrounding the "ring" and the cells in the area where nerves penetrate might also play a role in maintaining tissue integrity. Our observations are consistent with the hypothesis that cell migration likely plays a role during CVP placode formation.

There is still no molecular explanation for CVP placode morphogenesis into the "dome-like" structure observed (Fig. 1). In this study we attempted to clarify the molecular players that might participate during this process. It is known that nerve fibers enter the tongue mesenchyme starting from E11.5, but what is not known is how nerves find their way to particular sites of lingual epithelia, such as CVP or other gustatory papilla. One candidate that might be involved in this process is the extracellular matrices (ECM). The interactions between cells and the ECM are known to regulate many cellular functions, such as: cell proliferation, migration, morphogenesis and differentiation (Adams and Watt, 1993). Cell migration is among the major events that shape CVP morphogenesis, so components of the ECM might be the major molecular players that participate in this process.

The basement membrane is one example of the highly specialized ECM that lines the interface between epithelia and mesenchyme. Among all of the ECM glycoproteins, laminin is found predominantly in the basement membrane and is the first ECM expressed in the mammalian embryo (Martin and Timpl, 1987). Laminin has been shown to be involved in a variety of biological processes such as cell proliferation, cell migration, morphogenesis and cytodifferentiation (Klienman *et al.*, 1985; Aumailley and Smyth, 1998). Moreover, laminin had been shown to stimulate migration of neurons, promote axon extension and promote nerve regeneration (Calof and Lander, 1991; Clark *et al.*, 1993).

In our study, we observed a distinctive expression pattern of laminin during CVP morphogenesis. At the earliest developmental stage, the placode, laminin is distributed as a continuous thin line along the basement membrane. However, at latter developmental stages, as the nerves approach the basement membrane, laminin becomes more broadly distributed at the anterior portion of the placode and is decreased in apparent abundance in the area where the nerve will reach the basement membrane. At E13 when CVP morphology changes dramatically, laminin is intensely and broadly expressed in particular subsets of CVP epithelial cells (as shown in Fig. 3 C-H). However, in the "dome-shaped" structure, where nerves already occupy the central core, laminin is distributed as a continuous thin line along the basement membrane separating the epithelial from the underlying mesenchyme. The expression pattern for laminin appears to correlate with innervation and morphogenesis of the CVP, in that laminin is upregulated at sites where nerve fibers will penetrate into the CVP. It thus appears that innervation participates in the final morphogenetic steps of the CVP.

Mistretta and Haus (1996) previously reported laminin distribution during sheep gustatory papilla development. They showed that laminin is distributed continuously within the basement membrane, being interrupted only where taste buds form. In our study, we used SW mice, in which the taste buds will not differentiate until late E17 (State and Bowden, 1974). Discrepancies between our study and those of Mistretta and Haus (1996) may be due to animal species and developmental stage that we used. From our observations, laminin expression is highly regulated during CVP morphogenesis and innervation, suggesting that laminin may play a role in specifying an epithelial location where a nerve will penetrate thus providing innervation to taste anexa.

The results of this study suggest that 1) the CVP placode forms from the epithelial cells that migrate toward the midline; 2) E-cadherin may be down-regulated during cell migration to form a CVP placode; 3) laminin distribution may be involved in specifying

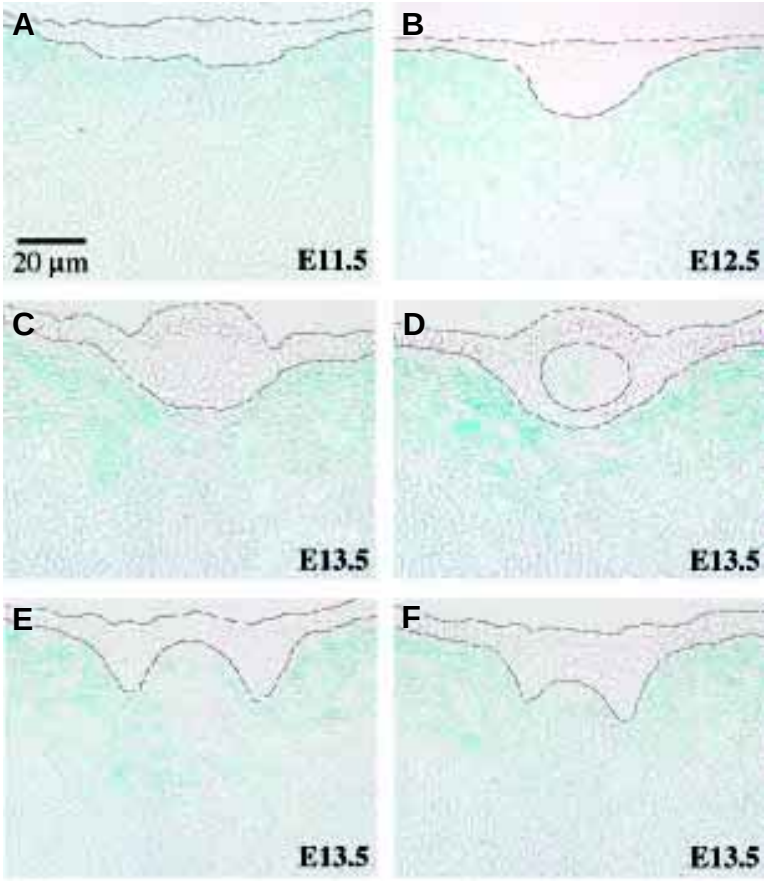

Fig. 6. Detection of the neural crest contribution to CVP development. *Lac Z staining of Wnt1-Cre/R26R reporter mouse embryos at E11.5* **(A)**, *E12.5* **(B)** *and E13* **(C-F)**. *The dashed lines define the epithelial outlines. The cells stained blue are neural crest derivatives. Bar, 20 μm for all images.*

the location and provide the guidance for the innervation of epithelial taste buds and 4) morphogenesis of the CVP is dependent upon innervation. Our study supports the observations of other investigators (Farbman and Mbiene, 1991; Oakley, 1993; Oakley *et al.*, 1993; Mbiene *et al.*, 1997; Morris-Wiman *et al.*, 1999) who suggest that maintenance of gustatory papilla morphology is nerve dependent, although initiation of gustatory papilla development is independent of nerve innervation.

Materials and Methods

Embryo Collection and Staging

Use of vertebrate animals complied with all institutional and federal guidelines. Timed pregnant Swiss-Webster mice were purchased from Charles River (Wilmington, MA). The mouse embryos were collected and staged according to somite pair (Theiler, 1989). Tissues from the posterior tongues of E12 to E15 embryos were dissected and fixed in Carnoy's solution (Ethanol:Chloroform:Glacial acetic acid = 6:3:1 v/v). Coronal plane of paraffin sections at 5 μm thickness were prepared and stored at 4° C until use. Scheme one demonstrates plane of section and terms used in the result and discussion.

Immunohistochemistry

Tissue sections were deparafinized in xylene and rehydrated in a graded series of ethanol solution (100%, 95%, 70% and 50% v/v). All processes were carried out at room temperature unless noted. After rehydration, the sections were submerged in 0.1 M phosphate buffered saline (PBS, pH 7.4), 2 times, 5 min each. Following treatment in 3% hydrogen peroxide in methanol to quench endogenous peroxidase, sections were treated with blocking solution provided by the manufacturer (Zymed). The sections were then incubated with primary-antibody: laminin (1:1000, Sigma), E-cadherin (1:1000, BD transduction laboratories), BrdU (1:200, Sigma), and PGP 9.5 (1:1000, Biogenesis), which was diluted in PBS containing 1% bovine serum albumin (BSA) overnight at 4°C. The following day, sections were washed three times, 10 min each, with 1x PBST (PBS, pH 7.4, 0.1% Tween 20) and then exposed to an appropriate biotinylated secondary antibody (Zymed) for 30 min. Sections were washed 3 times with PBST, incubated with the streptavidin-peroxidase conjugate for 15 min, and washed with PBST. The reaction product was detected by 3-amino-9-ethyl carbazole (AEC) substrate (Zymed). The red color indicates positive staining. Tissue sections were then mounted with glycerol vinyl alcohol (GVA) media.

Control tissue sections were incubated in the absence of primary antibody or in the absence of both primary- and secondary-antibody. In both cases no dye-complex was detected.

BrdU-Labeling and Staining

Bromo-deoxy-uridine (BrdU, 5'-Bromo-2'-deoxy-uridine, Sigma) was dissolved in PBS and administered into the intraperitonial cavity of timed pregnant mice at a dose of 100 μg/g body weight. The BrdU-labeled embryos were collected 4 hours after injection, washed twice in PBS and fixed in Carnoy's solution. The procedure for deparaffinization and to block endogenous peroxidase followed the same protocol as described above. Before exposing the tissue to the anti-BrdU antibody (Sigma), the DNA was depurinated by incubating the sections in 2 N HCl for 60 min at 37°C, then neutralized with 0.1 M Sodium borate pH 8.5 for 30 min and rinsed 4 times, 2 min each, with 1x PBST at room temperature. The non-specific binding of the antibody was blocked according to the manufacturer's protocol (Zymed). The sections were then incubated with 1:200 anti-BrdU antibody in 1% BSA in PBS at 4°C overnight. The reaction product was detected by AEC substrate-chromogen mixture (Zymed) and the sections were mounted with GVA mounting solution.

Control tissue sections were incubated in the absence of primary antibody or in the absence of both primary and secondary antibody. In both cases no dye-complex was detected.

Wholemount β-Galactosidase (X-gal) Staining

R26R conditional reporter mice are generous gifts from Dr. P. Soriano (Fred Hutchinson Cancer Research Center, Seattle, Washington). *Wnt-1* Cre transgenic mice are generous gifts from Dr. A. P. McMahon (Dept. of Molecular and Cellular Biology, Harvard University). Cross mating between the *Wnt-1* Cre transgenic mouse with the R26R conditional reporter transgenic mouse created double transgenic *wnt-1*-Cre/R26R mice which have been used to study the fate of neural crest cells (Chai *et al.*, 2000). The mice were euthanized and embryos from developmental stages E11.5 to E13 were collected. Genomic DNA was purified from each embryonic tail and subjected to genotypes by PCR. The 5' and 3' primer pairs used for detecting *Wnt1-Cre* gene in this study are primer 1 (5'-ATTCTCCCACCGTCAGTACG-3') and primer 2 (5'-CGTTTTCTGAGCA TACCTGGA-3') (Chai *et al.*, 2000). The R26R transgenic mice were genotyped according to Soriano (1999) (Soriano, 1999).

Tissues from the posterior tongues of each embryos were dissected and fixed in 4% paraformaldehyde at 4°C, 30 min. Tissues were washed with rinsing solution (2 mM $MgCl_2$ + 0.1% deoxycholic acid + 0.005% Nonidet P40 in 1x PBS) at room temperature, 2 times, 15 min each. After discarded the rinsing solution, tissues were incubated in X-gal staining solution (1 mg/mL of X-gal in 1x PBS containing 2 mM $MgCl_2$ + 0.1% deoxycholic acid + 0.005% Nonidet P40 + 35 mM potassium ferricyanide + 35 mM potassium ferrocyanide) at 37°C, overnight. Tissues were then refixed in 4% paraformaldehyde at room temperature for 1 hour, paraffin embedded and sectioned to observed lac-Z expression.

Acknowledgements

We thank Dr. P. Soriano and Dr. A.P. McMahon for the transgenic mice, Dr. Jun Han and Dr. Wen Luo for technical assistance, and Dr. Yi-Hsin Liu for critical reading and helpful comments on the manuscript. This work is supported by USPHS, NIH, National Institute of Dental and Craniofacial Research Grant # DE11834.

References

ADAMS, J.C. and WATT, F.M. (1993). Regulation of development and differentiation by the extracellular matrix. *Development* 117: 1183-1198.

AHPIN, P., ELLIS, S., ARNOTT, C. and KAUFMAN, M.H. (1989). Prenatal development and innervation of the circumvallate papilla in the mouse. *J. Anat.* 162: 33-42.

AUMAILLEY, M. and SMYTH, N. (1998). The role of laminins in basement membrane function. *J. Anat.* 193: 1-21.

BARASCH, J. (2001). Genes and proteins involved in mesenchymal to epithelial transition. *Curr. Opin. Nephro. Hypertens.* 10: 429-436.

CALOF, A.L. and LANDER, A.D. (1991). Relationship between neuronal migration and cell-substratum adhesion: Laminin and merosin promote olfactory neuronal migration but are anti-adhesive. *J. Cell Biol.* 115: 779-794.

CHAI, Y., JIANG, X., ITO, Y., BRINGAS, P., JR., HAN, J., ROWITCH, D.H., SORIANO, P., MCMAHON, A.P. and SUCOV, H.M. (2000). Fate of the mammalian cranial neural crest during tooth and mandibular morphogenesis. *Development* 127: 1671-1679.

CHUONG, C. (1993). The making of a feather: homeoproteins, retinoids and adhesion molecules. *Bioessays* 15: 513-521.

CLARK, P., BRITLAND, S. and CONNOLLY, P. (1993). Growth cone guidance and neuron morphology on micropatterned laminin surfaces. *J. Cell Sci.* 105: 203-212.

DE IONGH, R.U., LOVICU, F.J., OVERBEEK, P.A., SCHNEIDER, M.D., JOYA, J., HARDEMAN, E.D. and MCAVOY, J.W. (2001). Requirement for TGFβ receptor signaling during terminal lens fibers differentiation. *Development* 128: 3995-4010.

ECHELARD, Y., VASSILEVA, G. and MCMAHON, A.P. (1994). Cis-acting regulatory sequences governing *Wnt*-1 expression in the developing mouse CNS. *Development* 120: 2213-2224.

EKBLOM, P. (1989). Developmentally regulated conversion of mesenchyme to epithelium. *FASEB J.* 3: 2141-2150.

FARBMAN, A.I. and MBIENE, J.-P. (1991). Early development and innervation of taste bud-bearing papillae on the rat tongue. *J. Comp. Neurol.* 304: 172-186.

FRIEDRICH, G. and SORIANO, P. (1991). Promoter traps in embryonic stem cells: a genetic screen to identify and mutate developmental genes in mice. *Genes Dev.* 5: 1513-1523.

FRIXEN, U.H., BERHRENS, J., SACHS, M., EBERLE, G., VOSS, B., WARDA, A., LOCHNER, D. and BIRCHMEIER, W. (1991). E-cadherin-mediated cell-cell adhesion prevents invasiveness of human carcinoma cells. *J Cell Biol.* 113: 173-185.

GUMBINER, B.M. (1996). Cell adhesion: The molecular basis of tissue architecture and morphogenesis. *Cell* 84: 345-357.

HALL, J.M., HOOPER, J.E. and FINGER, E.F. (1999). Expression of *Sonic Hedgehog, Patched,* and *Gli* in developing taste papillae of the mouse. *J. Comp. Neurol.* 406: 143-155.

ISEKI, S., ARAGA, A., OHUCHI, H., NOHNO, T., YOSHIOKA, H., HAYASHI, F. and NOJI, S. (1996). Sonic hedgehog is expressed in epithelial cells during development of whisker, hair, and tooth. *Biochem. Biophys. Res. Commun.* 218: 688-693.

JERNVALL, J. and THESLEFF, I. (2000). Reiterative signaling and patterning during mammalian tooth morphogenesis. *Mech. Dev.* 92: 19-29.

JUNG, H.S., OROPEZA, V. and THESLEFF, I. (1999). *Shh*, *Bmp-2*, *Bmp-4* and *Fgf-8* are associated with initiation and patterning of mouse tongue papillae. *Mech. Dev.* 81: 179-182.

KLIENMAN, H.K., CANNON, F.B., LAURIE, G.W., HASSEL, J.R., AUMAILLEY, M., TERRANOVA, V.P., MARTIN, G.R. and DUBOIS-DALCQ, M. (1985). Biological activities of laminin. *J. Cell Biochem.* 27: 315-325.

MARTIN, G.R. and TIMPL, R. (1987). Laminin and other basement membrane components. *Annu. Rev. Cell Biol.* 3: 57-85.

MBIENE, J.-P., MACCALLUM, D.K. and MISTRETTA, C.M. (1997). Organ cultures of embryonic rat tongue support tongue and gustatory papilla morphogenesis *in vitro* without intact sensory ganglia. *J. Comp. Neurol.* 377: 324-340.

MISRETTA, C.M. and HAUS, L.F. (1996). Temporal and spatial patterns of tenascin and laminin immunoreactivity suggest roles for extracellular matrix in development of gustatory papillae and taste buds. *J. Comp. Morphol.* 364: 535-555.

MORRIS-WIMAN, J., BRINKLEY, L. and SEGO, R. (1999). An *in vitro* model for the study of the role of innervation in circumvallate papillae morphogenesis. *Dev. Brain Res.* 116: 141-150.

OAKLEY, B. (1993). The gustatory competence of the lingual epithelium requires neonatal innervation. *Dev. Brain Res.* 72: 259-264.

OAKLEY, B., LAWTON, A., RIDDLE, D.R. and WU, L.H. (1993). Morphometric and immunocytochemical assessment of fungiform taste buds after interuption of the chorda-lingual nerve. *Microsc. Res. Tech.* 26: 187-195.

PAULSON, R.B., HAYES, T.G. and SUCHESTON, M.E. (1985). Scanning electron microscopy study of tongue development in the CD-1 mouse fetus. *J. Craniofac. Genet. Dev. Biol.* 5: 59-73.

SHULER, C.F., HALPERN, D.E., GUO, Y. and SANK, A.C. (1992). Medial edge epithelium fate traced by cell lineage analysis during epithelial-mesenchymal transformation *in vivo. Dev. Biol.* 154: 318-330.

SJODIN, A., DAHL, U. and SEMB, H. (1995). Mouse R-cadherin: Expression during the organogenesis of pancreas and gastrointestinal tract. *Exp. Cell Res.* 221: 413-425.

SORIANO, P. (1999). Generalized lacZ expression with the ROSA26 Cre reporter strain. *Nat. Genet.* 21: 70-71.

SPIELMAN, A.I. and BRAND, J.G. (1995). Experimental cell biology of taste and olfaction. CRC press, Boca Raton.

STATE, F.A. and BOWDEN, R.E. (1974). Innervation and cholinesterase activity of the developing taste buds in the circumvallate papilla of the mouse. *J. Anat.* 118: 211-221.

THEILER, K. (1989). The house mouse: Atlas of embryonic development Springer Verlag, New York.

THESLEFF, I., VAAHTOKARI, A. and VAINIO, S. (1990). Molecular changes during determination and differentiation of the dental mesenchymal cell lineage. *J. Biol. Buccale* 18: 179-188.

THESLEFF, I., VAAHTOKARI, A., VAINIO, S. and JOWETT, A. (1996). Molecular mechanism of cell and tissue interactions during early tooth development. *Anat. Rec.* 245: 151-161.

THOMPSON, R.J., DORAN, J.F., JACKSON, P., DHILLON, A.P. and RODE, J. (1983). PGP 9.5-a new marker for vertebrate neurons and neuroendocrine cells. *Brain Res.* 278: 224-228.

WARBURTON, D., SCHWARZ, M., TEFFT, D., FLORES-DELGADO, G., ANDERSON, K.D. and CARDOSO, W.V. (2000). The molecular basis of lung morphogenesis. *Mech. Dev.* 92: 55-81.

WILKINSON, D.G., BAILES, J.A., CHAMPION, J.F. and MCMAHON, A.P. (1987). Expression of the proto-oncogene int-1 is restricted to specific neural cells in the developing mouse embryo. *Cell* 50: 79-88.

ZAMBROWICZ, B.P., IMAMOTO, A., FIERING, S., HERZENBERG, L.A., KERR, W.G. and SORIANO, P. (1997). Disruption of overlapping transcripts in the ROSA βgeo 26 gene trap strain leads to widespread expression of β-galactosidase in mouse embryos and hematopoietic cells. *Proc. Natl. Acad. Sci. USA*. 94: 3789-3794.

Received: February 2002
Reviewed by Referees: April 2002
Modified by Authors and Accepted for Publication: May 2002